Bacher.[14] It seems that the lines observed by Bacher did not appear in this discharge and none of those that did appear were favorable for such a calculation. Any estimate based upon these lines would be too large to be significant.

[14] R. F. Bacher, Phys. Rev. **43**, 1001 (1933).

In conclusion I wish to acknowledge the kindness of Professor H. C. Urey in supplying me with the sample of enriched nitrogen; furthermore, I wish to acknowledge my indebtedness to Professor F. A. Jenkins for his stimulating direction of my work.

JANUARY 1 AND 15, 1943 PHYSICAL REVIEW VOLUME 63

Dispersion of Elastic Waves in Solid Circular Cylinders*

G. E. HUDSON†
Department of Physics, Brown University, Providence, Rhode Island
(Received November 4, 1942)

The theory of elastic vibrations in solid circular cylindrical rods of homogeneous isotropic materials is redeveloped from the general equations of elasticity with the following general results: 1. For any mode of vibration the ratio of the velocity of any elastic wave traveling along the rod to the velocity c_0 of shear waves is the same for any two rods whose Poisson ratios are equal and whose ratios of circumference to shear wave-length are equal; 2. If the velocity of propagation for any particular mode remains less than c_0 as the frequency or radius is increased indefinitely, this velocity approaches that of Rayleigh surface-waves; 3. If the velocity of propagation for any particular mode remains greater than c_0 as the frequency or radius is increased indefinitely, this velocity approaches c_0 in the limit; and 4. A considerable simplification is introduced into the method of computing dispersion curves for any mode. This investigation not only generalizes and extends the work of D. Bancroft on elongational waves but further includes the computation of an exact table of dispersion curves for the flexural mode of vibration. The dispersion curves for magnesium are compared with the experimental results of Shear and Focke. Excellent agreement between theory and experiment is obtained for the first elongational and flexural branches.

INTRODUCTION

THE last few years have seen much progress, from both experimental[1] and theoretical[2–4] viewpoints, in the study of the phenomena associated with the vibrations of rods, particularly dispersion at high frequencies. Without exception, the exact theoretical treatments take as their starting points the solutions of the general dynamical equations of elasticity obtained originally by L. Pochhammer[5] for infinitely long rods. The most complete of these discussions is that of D. Bancroft,[2] who has calculated a table of velocities of elongational waves as a function of the ratio of the diameter of the rod to the wave-length for a wide range of values of Poisson's ratio.

An examination of experimental data reveals the existence of several types of rod vibrations often occurring either in conjunction with or to the exclusion of the elongational mode. This suggests the extension of the theoretical treatment to higher modes of vibration, to obtain dispersion curves for the associated elastic waves. Such calculations will be extremely useful in the future study of the stability and interaction of various modes of vibration and the study of the vibrations of a bar of finite length. The present article gives a general treatment of the problem of the propagation of longitudinally-traveling waves along a solid circular cylinder of infinite length, and presents a simplified method for the exact calculation of dispersion curves.

With a few important exceptions the quantities used in the analysis are similar to those

* Submitted in partial fulfillment of the requirements for the degree of Doctor of Philosophy at Brown University, Providence, Rhode Island.

† Now at the David Taylor Model Basin, Navy Department, Washington, D. C.

[1] S. K. Shear and A. B. Focke, Phys. Rev. **57**, 532 (1940).

[2] D. Bancroft, Phys. Rev. **59**, 588–593 (1941).

[3] E. Giebe and E. Blechschmidt, Ann. d. Physik **11**, 905 (1931); **18**, 417–485 (1933).

[4] G. S. Field, Can. J. Research **5**, 619–624 (1931); **8**, 563–574 (1933); **11**, 254–263 (1934).

[5] L. Pochhammer, J. f. d. reine u. angew. Math. (Crelle) **81**, 33–80 (1875).

introduced by Bancroft. The symbols denoting them are compared with Bancroft's in Table I.

TABLE I. Comparison of notations.

Symbol	Description	Bancroft's notation
$d=2a$	diameter of rod	d
α	$(1-2\sigma)/(1-\sigma)$; σ = Poisson's ratio	β
c	velocity of the wave	v
c_0	velocity of shear-waves $=(\mu/\rho)^{\frac{1}{2}}$	$v_0[2(1+\sigma)]^{\frac{1}{2}}$
z	$\frac{1}{2}(c/c_0)^2$	x
ν	frequency	v/L
τ_0	number of shear wave-lengths in a circumference $=\pi d\nu/c_0$	$\gamma av[2(1+\sigma)]^{\frac{1}{2}}/v_0$
x	$\tau_0[(2z-1)/2z]^{\frac{1}{2}}$	ka
y	$\tau_0[(\alpha z-1)/2z]^{\frac{1}{2}}$	ha
$\theta_\beta(\xi)$	$\xi J_\beta'(\xi)/J_\beta(\xi)$	
$\theta_1(\xi)+1$	$\xi J_0(\xi)/J_1(\xi)=-\xi^2/\theta_0(\xi)$	$\phi(\xi)$

THEORY AND CALCULATIONS

We choose solutions of the differential equations of motion in the form of expressions for the components of the displacement vector $\mathbf{u}$ which represent a wave traveling along the axis of the rod (the ζ axis), and which are single-valued functions of the cylindrical coordinates r, θ, ζ. By imposing the boundary condition on these solutions, that the stress vector vanish at the lateral surface, we find the infinite set of secular equations, defining c/c_0 as a function of τ_0,

$$0=\begin{vmatrix} \left\{\beta^2-y^2-\frac{1}{2}\tau_0^2\frac{\sigma}{1-\sigma}\right\}J_\beta(y)-yJ_\beta'(y), & 2\beta\{xJ_\beta'(x)-J_\beta(x)\}, & \{\beta^2-x^2\}J_\beta(x)-xJ_\beta'(x) \\ \beta\{yJ_\beta'(y)-J_\beta(y)\}, & \{2\beta^2-x^2\}J_\beta(x)-2xJ_\beta'(x), & \beta\{xJ_\beta'(x)-J_\beta(x)\} \\ yJ_\beta'(y), & \beta J_\beta(x), & (1-z)xJ_\beta'(x) \end{vmatrix}, \quad (1)$$

where β takes on any integral value, and in this way determines the mode of vibration. This form naturally suggests the introduction of the θ_β functions (cf. Table I), by dividing (1) by $J_\beta^2(x)\cdot J_\beta(y)$. After some manipulation, (1) becomes

$$0=\begin{vmatrix} \beta^2-1-x^2(z-1)/(2z-1), & 2(\beta^2-1)\theta_\beta(x)-x^2, & \beta^2-1-x^2 \\ -1, & \beta^2-2\theta_\beta(x)-x^2, & z\theta_\beta(x)-1 \\ \theta_\beta(y), & \beta^2, & (1-z)\theta_\beta(x) \end{vmatrix}. \quad (2)$$

As has been recognized by Field and Bancroft, the function c/c_0 of τ_0 defined by the secular Eqs. (1) or (2) is not always single-valued, but in certain cases may have many branches. This is true in particular of the elongational and torsional modes, obtained when $\beta=0$. However, it is not the case for the flexural mode, whose dispersion curve consists of just one branch. It should be pointed out here that there is some experimental evidence for the existence of the higher branches of the elongational or torsional modes (cf. Figs. 2 and 3).

In order to discuss the calculation of the dispersion curves obtainable from this set of equations, it is necessary first to investigate some properties of the θ_β functions.

As a consequence of the recursion relations satisfied by the Bessel functions $J_\beta(\xi)$ the θ_β functions satisfy the non-linear recursion relations

$$[\theta_\beta(\xi)-\beta]=\frac{-\xi^2}{2(\beta+1)+[\theta_{\beta+1}(\xi)-(\beta+1)]}. \quad (3)$$

From this, it follows immediately that we can develop the functions into the infinite continued fraction

$$\theta_\beta(\xi)-\beta=\frac{-\xi^2}{2(\beta+1)+}\,\frac{-\xi^2}{2(\beta+2)+}\cdots\frac{-\xi^2}{2(\beta+n)+}\cdots, \quad (4)$$

which can be shown to converge to

$$[\xi\{J_\beta'(\xi)/J_\beta(\xi)\}-\beta]$$

for all real and imaginary values of ξ. It is seen that the value of the function $\theta_\beta(\xi)$ for a particular ξ can be approximated as closely as we wish by taking a large enough number of components of the continued fraction expansion (4). This computation proceeds very quickly on a

modern high speed calculator; to calculate $\theta_1(\xi)$ correct to nine places, it is only necessary to perform twelve successive divisions for values of $|\xi|$ as large as 5.0.

For both real and imaginary arguments we have, when $|\xi|$ is small,

$$\theta_\beta(\xi) \doteq \beta - \xi^2/[2(\beta+1)]$$

and, for any ξ, as β becomes large,

$$\theta_\beta(\xi) \doteq \beta.$$

When ξ is imaginary,

$$\theta_\beta(\xi) \doteq -i\xi - \tfrac{1}{2},$$

when $|\xi|$ takes on large values, while for ξ real,

$$\theta_\beta(\xi) \doteq \xi \cot [\xi - \tfrac{1}{4}(2\beta-1)\pi],$$

as $|\xi|$ becomes great.

From the approximate expressions for the θ_β functions, it is easy to show by substitution into (2) that, when the frequency or the rod-diameter is small enough so that τ_0 is very small, we have the approximate secular equation

$$0 \doteq a_0(z, \alpha, \beta) + a_1(z, \alpha, \beta)\tau_0^2 + a_2(z, \alpha, \beta)\tau_0^4, \quad (5)$$

in which

$$a_0 = 8z\beta(\beta+1)(\beta^2-1)\{z(\alpha-2)+1\},$$
$$a_1 = -4z(\beta+1)\{z(\alpha-2)(2\beta-1)-(2\alpha-3)(\beta-1)\},$$
$$a_2 = (2z-1)\{z(\alpha-2)-(2\alpha-3)\},$$

for the velocity ratio c/c_0 as a function of τ_0. For higher modes of vibration, β is very large, and the velocity becomes accordingly

$$c = c_0[2(1-\sigma)]^{\frac{1}{2}},$$

when τ_0 is small. As far as the author is aware, waves of this velocity have never been observed.

TABLE II. Minimum velocity ratios and asymptotic behavior of elongational wave dispersion curves.

σ	$(c/c_0)_{\min}$	$(\tau_0)_{\min}$	$(c/c_0)_{\tau_0=\infty}$	$\left(\frac{c}{c_0}\Big/\frac{1}{\tau_0}\right)_{\tau_0=\infty}$
0.00	0.855557	7.33337	0.8740320	−0.2173949
0.10	0.881559	9.05149	0.89310	−0.172540
0.15	0.893279	10.1115	0.90223	−0.151562
0.20	0.904174	11.3470	0.91099	−0.131860
0.25	0.914277	12.8025	0.91940	−0.113543
0.30	0.923626	14.5362	0.92742	−0.0967458
0.35	0.932264	16.6270	0.93501	−0.0815527
0.40	0.940233	19.1850	0.94220	−0.0679408
0.50	0.954375	26.4389	0.9553125	−0.04535197

On the other hand, if, as τ_0 is increased indefinitely, the wave velocity of some mode of vibration remains less than c_0, then this velocity c is obtainable from

$$(1-z)^2 = (1-\alpha z)^{\frac{1}{2}}(1-2z)^{\frac{1}{2}}. \quad (6)$$

This equation is identical, except for a change in notation, with the equation for the velocities of Rayleigh's surface waves in an infinite medium.[6] Similarly, if c remains greater than c_0 for some mode, it is seen that this velocity must approach c_0 in the limit as the product of frequency and rod-diameter approaches infinity. To apply these deductions, then, it is necessary to determine which modes have velocities greater or less than c_0 as τ_0 becomes large. Hence, we find the largest root, τ_0, of the equation obtained from (2) by letting $z \to \frac{1}{2}$, i.e., $c \to c_0$, *viz.*,

$$0 = \frac{\tau_0^4}{4}\left(\frac{\beta-1}{\beta+1}\right) + \frac{\tau_0^2}{2}(2\beta-3)[\beta-\theta_\beta(y)] + \beta(\beta^2-1)[\beta-\theta_\beta(y)], \quad (7)$$

where $y^2 = \tau_0^2(\alpha-2)/2$. Then if the slope of the dispersion curve in the $(\tau_0, c/c_0)$-plane is negative at this root, the velocity becomes less than c_0, and conversely.

When β is set equal to zero in (2), the secular determinant factors into the product of two expressions, which, when set equal to zero in turn, give the equations of the dispersion curves of torsional and elongational waves, respectively. These become identical with the equations given by Bancroft for these modes if we introduce the change of notation indicated in Table I. However, Bancroft's results and calculations for elongational waves may be extended as follows. By taking the asymptotic expansion for $\phi(\xi)$, ξ imaginary, valid for large $|\xi|$, we find near $\tau_0 = \infty$ that the elongational curve has the slope

$$\left[\frac{d(c/c_0)}{d(1/\tau_0)}\right]_{\tau_0=\infty} = \frac{(1-z)^2-(1-z)^4}{(1-2z)^{\frac{1}{2}}\{\alpha/2+(1-z)^4-2(1-z)\}}, \quad (8)$$

where z is determined by (6).

[6] Lord Rayleigh, Proc. London Math. Soc. **17**, 4–11 (1885).

TABLE III. Flexural wave dispersion curves for various values of Poisson's ratio.

$\tau_0 =$	$\sigma=0.00$	0.10	0.15	0.20	0.25	0.30	0.35	0.40	0.50
0.0	0.0000000	0.0000000	0.0000000	0.0000000	0.0000000	0.0000000	0.0000000	0.0000000	0.0000000
0.2	.3555010	.3640608	.3681160	.3720349	.3758288	.3795038	.3830692	.3865318	.3931709
0.4	.4775240	.4889918	.4944082	.4996310	.5046750	.5095520	.5142708	.5188420	.5275762
0.6	.5576783	.5710290	.5773082	.5833474	.5891622	.5947667	.6001742	.6053962	.6153268
0.8	.6160680	.6307710	.6376520	.6442482	.6505770	.6566550	.6624978	.6681200	.6787528
1.0	.6608194	.6765492	.6838712	.6908618	.6975420	.7039325	.7100500	.7159128	.7269328
1.2	.6961910	.7127362	.7203908	.7276680	.7345922	.7411860	.7474712	.7534670	.7646630
1.4	.7247312	.7419508	.7498658	.7573562	.7644502	.7711738	.7775522	.7836090	.7948402
1.6	.7480972	.7658980	.7740240	.7816770	.7888910	.7956950	.8021174	.8081858	.8193600
1.8	.7674272	.7857478	.7940542	.8018392	.8091400	.8159908	.8224248	.8284742	.8395332
2.0	.7835359	.8023430	.8108092	.8187060	.8260740	.8329519	.8393790	.8453910	.8563025
2.2	.7970260	.8163020	.8249200	.8329180	.8403432	.8472390	.8536492	.8596158	.8703660
2.4	.8083570	.8280960	.8368642	.8449620	.8524408	.8593510	.8657432	.8716620	.8822500
2.6	.8178838	.8380912	.8470120	.8552120	.8627478	.8696760	.8760512	.8819258	.8923618
2.8	.8258888	.8465730	.8556530	.8639628	.8715628	.8785152	.8848820	.8907188	.9010172
3.0	.8326003	.8537732	.8630212	.8714494	.8791232	.8861100	.8924768	.8982860	.9084667
3.2	.8382070	.8598770	.8693030	.8778620	.8856208	.8926532	.8990318	.9048250	.9149098
3.4	.8428650	.8650388	.8746530	.8833530	.8912110	.8983020	.9047048	.9104942	.9205070
3.6	.8467108	.8693870	.8791982	.8880520	.8960212	.9031842	.9096252	.9154230	.9253888
3.8	.8498592	.8730310	.8830460	.8920648	.9001572	.9074062	.9138980	.9197190	.9296608
4.0	.8524131	.8760632	.8862868	.8954793	.9037082	.9110556	.9176120	.9234680	.9334112
4.2	.8544618	.8785662	.8889990	.8983722	.9067470	.9142062	.9208400	.9267438	.9367120
4.4	.8560860	.8806110	.8912502	.9008090	.9093398	.9169202	.9236438	.9296070	.9396230
4.6	.8573530	.8822620	.8931022	.9028468	.9115390	.9192510	.9260752	.9321100	.9421950
4.8	.8583318	.8835750	.8946062	.9045352	.9133930	.9212442	.9281788	.9342960	.9444688
5.0	.8590708	.8846020	.8958110	.9059189	.9149430	.9229395	.9299930	.9362010	.9464833

Further, an extended analysis shows that the elongational curve for a certain α has a minimum lying on the locus defined by

$$\phi\left[i\frac{\tau_0}{(2z)^{\frac{1}{2}}}\left(\frac{1-z}{\phi(x)-z}\right)b\right]=\frac{b^2}{\phi(x)-z}, \tag{9}$$

where

$$b^2=\phi^2(x)-2z+\tfrac{1}{2}\tau_0{}^2z.$$

Corresponding to each point (τ_0, z) on this locus, there is a dispersion curve defined by a particular α which has this point as a minimum. α is obtained from

$$\alpha=\frac{1}{z}\left[1-\left(\frac{1-z}{\phi(x)-z}\right)^2 b^2\right]. \tag{10}$$

Table II gives the values at $\tau_0=\infty$ of the velocity ratio c/c_0, and the slope, $[d(c/c_0)/d(1/\tau_0)]$, calculated from (6) and (8) for various values of σ, Poisson's ratio. Also included in this table is a list of coordinates, calculated from (9) and (10), of the minima of those elongational curves characterized by these same values of σ.

Let us now turn to a consideration of the flexural modes of motion. If we give β the value unity in (2), define

$$\psi(\xi)=\theta_1(\xi)-1, \tag{11}$$

and reduce the resulting secular determinant of order three to one of order two by the pivotal method, there results the equation,

$$0=\begin{vmatrix} \psi(y)(1-2z)+(1-z)\{2\psi(x)+x^2\}, & \\ & -3\psi(x)-x^2 \\ \psi(y)(1-2z)-z, & -(1-z)\psi(x)+z \end{vmatrix}, \tag{12}$$

of the dispersion curve of the flexural waves. It is possible to show that, for a given value of Poisson's ratio, this curve has contact of the first order, but not higher, at $\tau_0=\infty$ with the lower branch of the dispersion curves of the elongational waves, characterized by the same value of σ. Equation (7), with $\beta=1$, gives a good approximation to the flexural wave dispersion curves provided τ_0 is not too large.

Table III, accurate to six places, is the result of calculating, by (12), c/c_0 as a function of τ_0 and σ for flexural waves. It should be emphasized again that the units used in the construction of this table are not the same as those in Bancroft's table for elongational waves. Conversion formulae between the two forms of tables are easily obtained from the list of symbols given in Table I. Bancroft's units are convenient if Young's modulus E is known accurately; the units τ_0 and

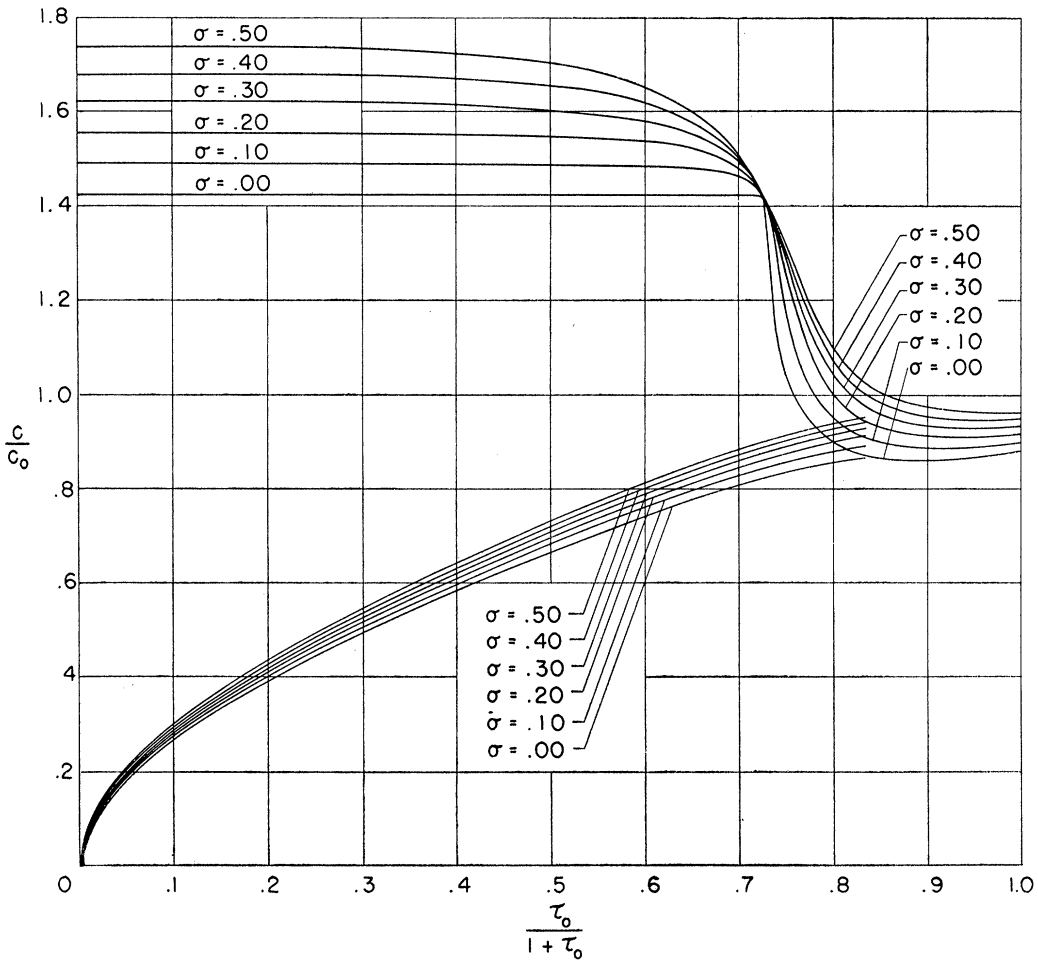

FIG. 1. Theoretical elongational wave dispersion curves (upper family) and flexural wave dispersion curves (lower family) for various values of Poisson's ratio.

c/c_0 are more convenient to the experimenter if the shear modulus is known accurately, or if the constant velocity c_0 of torsional waves is obtained from an experiment. c_0 constitutes a natural reference velocity at *any* frequency at which an experiment on the propagation of waves in rods is being conducted.

Figure 1 shows the comparison in the units of $(\tau_0, c/c_0)$ between the family of elongational wave dispersion curves computed by Bancroft, and the flexural wave dispersion curves presented in Table III. For convenience, the variable $\tau_0/(1+\tau_0)$ is plotted as abscissa, rather than τ_0 itself. This serves to emphasize the minima of the elongational curves as well as the slopes at $\tau_0=\infty$. Note the universal point, $c/c_0=1.4142\cdots$, $\tau_0=2.6038\cdots$, at which all the elongational curves are tangent. This point is quite helpful in obtaining rough estimates of the shape of curves in the elongational family. It appears from this figure that the flexural curves have very slight maxima for certain large values of τ_0. A calculation of these maxima would be interesting to carry out.

COMPARISON WITH EXPERIMENT

For the purpose of comparing theory and experiment, Shear's data[1] for two magnesium rods (machined sticks) with diameters equal to 5.895 mm and 4.615 mm, and two silver rods (hard-drawn) with diameters 5.009 mm and 4.061 mm, were recomputed in the units of τ_0

and c/c_0. For magnesium, c_0 was chosen as 30.97×10^4 cm/sec., while for silver, c_0 was taken as 15.78×10^4 cm/sec.

Figure 2 shows the data for the magnesium rods compared with the theoretical curves for $\sigma=0.25$. It is seen that both the flexural and elongational curves agree well with the data for both rods except for a few isolated points, which probably lie on curves corresponding to higher order modes of vibration.

Figure 3 illustrates the effect of non-isotropy resulting from the hard-drawing treatment of the silver rods. The data for both rods are compared with the theoretical curves for $\sigma=0.39$ and $\sigma=0.49$. The flexural mode agrees best with the choice $\sigma=0.49$ for the theoretical curve whereas the choice $\sigma=0.39$ for the theoretical curve is

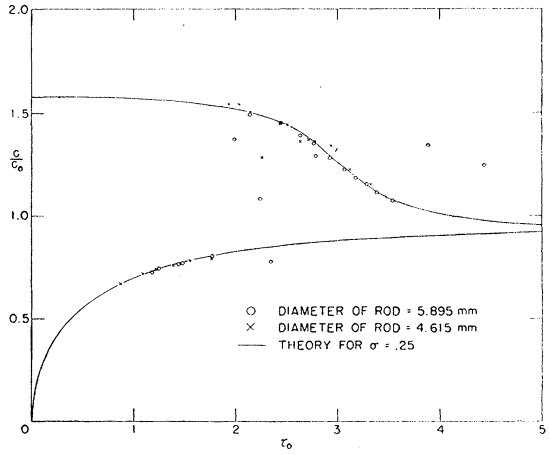

FIG. 2. Experimental data for magnesium rods compared with the theoretical curves for $\sigma=0.25$.

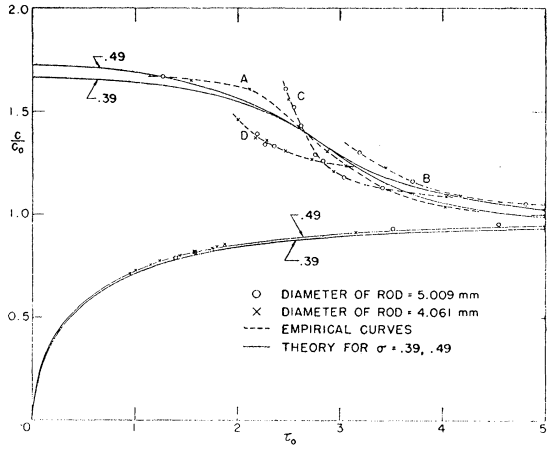

FIG. 3. Experimental data for hard-drawn silver rods compared with the theoretical curves for $\sigma=0.39$ and 0.49.

closer to the empirical curve for elongational waves, denoted by the dashed line A. However, this latter agreement is not at all as good as it is for the flexural branch; it appears that no choice of σ can bring about agreement in the shapes of the curves. This difference in shape, then, is one of the effects of non-isotropy which would have to be derived from a theory of non-isotropic rod vibrations. The dashed empirical curves B, C, and D are likely due to the presence of higher modes of vibration.

The author wishes to express his thanks to Professor R. B. Lindsay for his many useful suggestions throughout the research, and to Professor W. Feller for his helpful suggestions concerning the practical computational procedure.